Crystal growth and spectral properties of $(Yb_{0.15}Lu_{0.85x}Y_{0.85-0.85x})_3Al_5O_{12}$ single crystals

Ruifeng Tian (田瑞丰) [1, 2], Mingyan Pan (潘明艳) [1*] , Lu Zhang (张璐) [1,2], Hongji Qi (齐红基) [1]**

[1] Key Laboratory of Materials for High Power Laser, Shanghai Institute of Optics and Fine Mechanics, Chinese Academy of Sciences, Shanghai 201800, China

[2] University of Chinese Academy of Sciences, Beijing, P.R. 100049, China

[*]Correspondence Author:

pmy@siom.ac.cn; [**]Correspondence Author: qhj@siom.ac.cn

Abstract

Four single crystals $(Yb_{0.15}Lu_{0.85x}Y_{0.85-0.85x})_3Al_5O_{12}$ (x=0, 0.25, 0.5, 1) were grown by the Czochralski method. The correlation of the host atom Lu:Y ratios with the density and the luminescence properties were revealed. The density increases linearly with increasing of Lu^{3+} content, which will improve the gamma ray cut-off ability. The integrated intensity of the XEL spectrum increases exponentially with increasing the Y:Lu ratio. While the decay time becomes even shorter with increasing the Lu^{3+} content. These results will provide a basis to balance the comprehensive properties to match different application requirements.

Keywords: Yb:LuYAG; scintillators; Czochralski method; Charge transfer.

1. Introduction

Inorganic scintillation crystals are widely used in high-energy particle detection, medical imaging, nuclear physics and other fields[1]. Due to the development of high energy physics and ultrafast pulsed radiation detection, the demand for ultrafast scintillators is becoming more and more urgent.

Ytterbium-doped yttrium aluminum ($Yb:Y_3Al_5O_{12}$, Yb:YAG) is a traditional material with excellent comprehensive performance, such as good thermal conductivity, optical performances, excellent chemical stability, etc. Up to now, Yb:YAG crystals have been widely used as high-power laser materials[2-4]

Besides, Yb:YAG is also a very important inorganic scintillator since it possesses an ultrafast decay time (0.41ns excited by 266nm pulsed laser)[5], which shows potential applications in pulsed radiation imaging, the inertial confinement fusion (ICF) diagnosis, nuclear reaction kinetics diagnosis, and homeland security.[6-9]

The study of Yb:YAG scintillators started from 1997, Raghavan et al. reported that 15 wt% Yb can be used to detect low-energy solar neutrinos[10]. In 2000, L. van Pieterson et al. systematically studied the charge-transfer luminescence behavior of Yb ions in different compounds, and estimated the thermal quenching temperature of Yb:YAG at T=80 K[11]. In 2001, N. Guerassimova et al. reported the X ray excited charge transfer luminescence at T=80 K. The luminescence peaks at 333 nm and 500 nm belong to charge transfer (CT) luminescence based on the luminescence spectrum[12]. The CT state refers to the transfer process of electrons from oxygen ligands to rare earth ions (Yb^{3+}). CT luminescence refers to the energy transfer from the CT state two the energy levels of $^2F_{7/2}$ and $^2F_{5/2}$. The Stokes shift of the CT state is 17500 cm^{-1} reported by van Pieterson et al.[11]. While P. Antonini et al. reported that dependency between light yield (LY) and temperature. More detail, the maximum light yield is $(13.5\pm2.5)\times10^3$ ph/MeV at 140 K for 25% Yb:YAG and the decay time τ is shorter than 4 ns under the γ source[13].

Since Yb:YAG features extremely low light yield in comparison with commercial scintillators like BGO, Ce:LYSO etc, it is only suitable in the application of high intensity pulsed gamma ray measurement. In previous studies, Kan Zhang[7] reported that the fluence rate linear response upper limit of the Yb:YAG

crystal is about 9.1×10^{18} MeV·cm^{-2}·s^{-1}, and the sensitivity of Yb:YAG detector is 6.16×10^{20} C·cm^{-2}·MeV^{-1}. In order to further improve the detecting capacity, the gamma ray cut-off ability and the radiation hardness of Yb:YAG single crystal should be improved.

Preliminary studies have shown that doping of host elements can modulate the crystal scintillation properties. The Ce:LuAG has better energy resolution (6.7±0.3%) than Ce:YAG, while the scintillation decay time show a longer slow component for the Ce:LuAG respect to the Ce:YAG[14]. The Ce:LYSO has higher light yield (37400±3700 ph/MeV) but the worse energy resolution (7.7±0.2%) respect to the Ce:YSO[15]. Thus, we can conclude that Y-Lu solid solute plays a huge role in the improvement of scintillator properties. However, Yb doped YAG-LuAG solid solute have not been investigated systematically.

Therefore, in order to regulate the density and explore the relationship between the host atom substitution in Yb:LuYAG system and spectral properties, we grow the single crystals of $(Yb_{0.15}Lu_{0.85x}Y_{0.85-0.85x})_3Al_5O_{12}$ (x=0, 0.25, 0.5, 1) by Czochralski method. With the same valent state and similar atom size, Lu^{3+} can substitute Y^{3+} with an arbitrary value ranging from 0 to 100 at.%. The atom concentration of Yb is 15% in all the crystals. Due to the extremely low LY of Yb:YAG crystals, the spectrally integrated intensities of X-ray excited luminescence (XEL) spectra are widely used to evaluate their LY at room temperature. Thus, the XEL properties and decay time of the crystals were characterized and analyzed in detail.

2. Experimental procedure

$(Yb_{0.15}Lu_{0.85x}Y_{0.85-0.85x})_3Al_5O_{12}$ (x=0, 0.25, 0.5, 1) crystals were grown by Czochralski method with a mid-frequency induction heating system. The raw materials were high-purity Yb_2O_3 (5N purity), Y_2O_3 (5N purity), Al_2O_3 (5N purity) and Lu_2O_3 (5N purity). The stoichiometry of starting materials was weighed accurately under the formula $(Yb_{0.15}Lu_{0.85*x}Y_{0.85-0.85x})_3Al_5O_{12}$ (x=0, 0.25, 0.5, 1). The crystals were grown with <111> orientation in Ar atmosphere. General cylindrical shape of the as grown $(Yb_{0.15}Lu_{0.85x}Y_{0.85-0.85x})_3Al_5O_{12}$ (x=0.25, 0.5, 1) is shown in FIG. 1. The crystals grow in an oxygen-deficient environment with a high concentration of oxygen vacancies. Annealing in the air can reduce the defect density and remove the thermal stress during the growth. All crystals were annealed at 1200 ℃ for 12 hours. The as-grown crystals were blue and changed to colorless after annealing process. The crystals were cut and polished for the optical measurements, the size of the sample is 10*10*1 mm (FIG. 2).

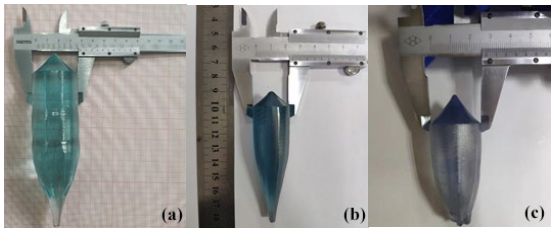

FIG. 1. The picture of the as grown crystals for $(Yb_{0.15}Lu_{0.2125}Y_{0.6375})_3Al_5O_{12}$ (a), $(Yb_{0.15}Lu_{0.425}Y_{0.425})_3Al_5O_{12}$ (b), $(Yb_{0.15}Lu_{0.85})_3Al_5O_{12}$ (c).

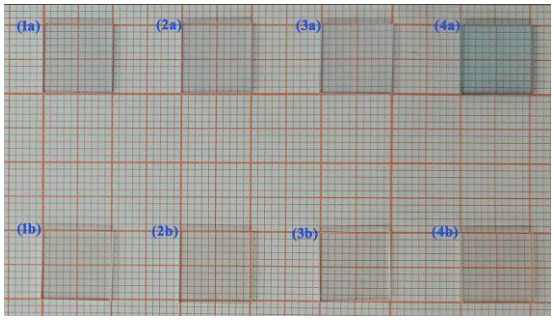

FIG. 2. The picture of the crystals for $(Yb_{0.15}Y_{0.85})_3Al_5O_{12}$ (1a, 1b), $(Yb_{0.15}Lu_{0.2125}Y_{0.6375})_3Al_5O_{12}$ (2a, 2b), $(Yb_{0.15}Lu_{0.425}Y_{0.425})_3Al_5O_{12}$ (3a, 3b), $(Yb_{0.15}Lu_{0.85})_3Al_5O_{12}$ (4a, 4b). The samples in first and second row are before and after annealing, respectively.

The density values of the four samples were measured using the Archimedes method. The optical properties were performed by a PerkinElmer Lambda 1050 UV/VIS/NIR Spectrometer (Massachusetts, USA). XEL spectra and decay time by pulse laser at 213 nm profiles were carried by a luminescence spectrometer (Edinburgh Instrument FLS1000, Edinburgh, UK). The X-ray source with Ag target operating at 50 kV and 15 μA was used as an excitation source. The pulse width of the pulse laser at 213 nm is 43.102 ps.

3. Results and discussion

The density of single crystals for $(Yb_{0.15}Lu_{0.85x}Y_{0.85-0.85x})_3Al_5O_{12}$ (x=0, 0.25, 0.5, 1)

were shown in Table 1. The density increases linearly with increasing of Lu^{3+} content, which is consistent with Equation (1) and the Adjusted R^2=0.99668.

$$y=a+b\cdot x \quad (1)$$

where intercept a=4.872, slope b=1.907.

Table 1. The densities of the single crystals for $(Yb_{0.15}Lu_{0.85x}Y_{0.85-0.85x})_3Al_5O_{12}$ (x=0, 0.25, 0.5, 1) .

Sample	Density (g/cm^3)
$(Yb_{0.15}Y_{0.85})_3Al_5O_{12}$	4.83
$(Yb_{0.15}Lu_{0.2125}Y_{0.6375})_3Al_5O_{12}$	5.40
$(Yb_{0.15}Lu_{0.425}Y_{0.425})_3Al_5O_{12}$	5.83
$(Yb_{0.15}Lu_{0.85})_3Al_5O_{12}$	6.77

Transmission spectra as a function of incident wavelength (200–1200 nm) for $(Yb_{0.15}Lu_{0.85x}Y_{0.85-0.85x})_3Al_5O_{12}$ (x=0, 0.25, 0.5, 1) single crystals annealed in air are shown in FIG. 3. It can be seen that the transmittance curves of these samples are similar in the range of 300-1200 nm, and the transmittance has been maintained around 80% in the range of 300–878 nm. The absorption bands of Yb^{3+} were centered at 940 nm corresponding to the 4f-4f transition. There is no significant difference in the absorption curves for the four samples near 940 nm. The absorption of the single crystals for $(Yb_{0.15}Lu_{0.85x}Y_{0.85-0.85x})_3Al_5O_{12}$ (x=0，0.25, 0.5, 1) below 300 nm is related to the defects and impurity in the crystals[16]. The absorption band near 255 nm which is believed to arise from O^{2-} to Fe^{3+} charge transfer[17]. According to the research of D. Fagundes-Peters et al.[18], Fe^{3+} impurities are usually unavoidable, which were caused by iridium crucible and growth environment. The Fe^{3+} ion will occupy the tetrahedral and octahedral Al^{3+} sites in the lattice[19], and a small amount of Fe^{3+} can seriously affect the induced optical losses after ultraviolet irradiation[20]. As shown in FIG. 3, $(Yb_{0.15}Lu_{0.2125}Y_{0.6375})_3Al_5O_{12}$ has the highest transmittance near 255 nm, which needs further study.

The Lu^{3+} occupy the Y^{3+} site in the $(Yb_{0.15}Lu_{0.85x}Y_{0.85-0.85x})_3Al_5O_{12}$ crystal, and the radius of the Lu^{3+} (radius=0.083 nm) is smaller than that of the Y^{3+} (radius=0.090 nm), resulting in a smaller ligand size around the oxygen[21, 22]. Therefore, the energy of the electron transfer from the oxygen ligand to the rare earth ions increases, and the CT absorption band will appear blue-shifted.

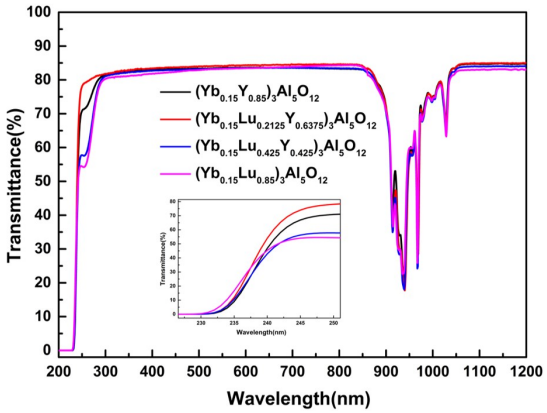

FIG. 3. Transmittance of the single crystals for $(Yb_{0.15}Lu_{0.85x}Y_{0.85-0.85x})_3Al_5O_{12}$ (x=0, 0.25, 0.5, 1).

FIG. 4 shows the XEL spectra of crystals for $(Yb_{0.15}Lu_{0.85x}Y_{0.85-0.85x})_3Al_5O_{12}$ (x=0, 0.25, 0.5, 1) at room temperature. The luminescence band near 330 nm and 500 nm corresponds to the transition from CT state to $^2F_{7/2}$ ground state and to $^2F_{5/2}$ excited state. The result is consistent with the report of Guerassimova et al.[12] . According to the position of the emission peaks in the XEL spectrum, the energy separation between $^2F_{7/2}$ and $^2F_{5/2}$ is 9761 cm^{-1} for all the samples. The energy separation is higher than 9300 cm^{-1} measured at 80 K reported by Nikl et al.[23], possibly due to the increase of temperature.

According to FIG. 4, the luminescence intensity of the sample gradually increases with the increase of Y^{3+} concentration, which may be related to the concentration of the defect in the crystals[24]. There is a non-stoichiometric growth phenomenon during the growth of YAG single crystal[26]. The existence of Y_{Al} antisite defect is beneficial to the composition deviation to restore equilibrium. The antisite defects will lead to an increase in the volume of octahedral sites in the lattice[27]. Therefore the covalency of the lattice will increase. This leads to the splitting of energy levels at the bottom of the conduction band, resulting in localized energy levels in the band gap. These localized energy levels act as carrier traps, which adversely affect the scintillation process[28]. The antisite defects concentration in the crystal is related to the radius of rare

earth ions and melting point. The defects concentration increases with decreasing the rare earth ion radius[17, 29]. According to Zorenko et al., no antisite defects were observed in Ce: YAG single crystal films (SCF) samples prepared at low temperatures[31]. Therefore, the antisite defect concentration may increase with increasing crystal growth temperature. The melting point of the $(Yb_{0.15}Lu_{0.85x}Y_{0.85-0.85x})_3Al_5O_{12}$ increases with the Lu^{3+} concentration[32]. Thus the crystals with higher Lu^{3+} concentrations have higher concentrations of the antisite defects.

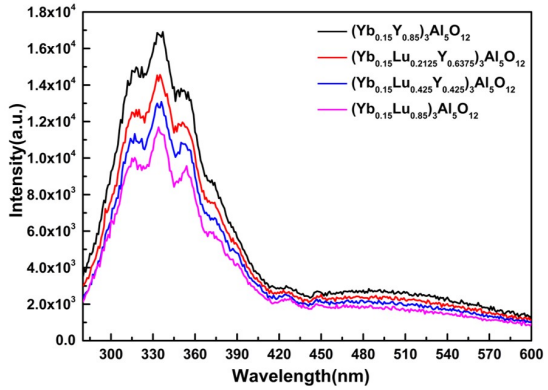

FIG. 4. XEL spectra of the single crystals for $(Yb_{0.15}Lu_{0.85x}Y_{0.85-0.85x})_3Al_5O_{12}$ (x=0, 0.25, 0.5, 1) at room temperature.

The relationship between Lu^{3+} concentration and XEL integrated intensity in the range of 280 nm-400 nm is shown in FIG. 5. The black dot plot is the integral intensity with $(Yb_{0.15}Lu_{0.85x}Y_{0.85-0.85x})_3Al_5O_{12}$, and the red curve is the fitting result. The integral intensity decreases exponentially with increasing of Lu^{3+} content in the range of 280 nm-400 nm, which is consistent with Equation (2) and the Adjusted R^2=0.99922.

$$y=y_0+A\cdot exp(R_0\cdot x) \quad (2)$$

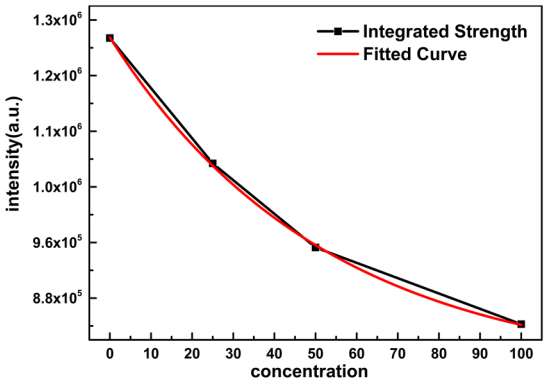

FIG. 5. Luminescence integral intensity varies with Lu^{3+} concentration increase.

The $(Yb_{0.15}Lu_{0.85x}Y_{0.85-0.85x})_3Al_5O_{12}$ decay time were shown in FIG. 6. All decay curves follow single-term exponential Equation (3):

$$I(t)=I_0\cdot exp(-t/\tau) \quad (3)$$

Where I_0 is the intensity at zero time, τ is decay time.

The decay time values of the single crystals for $(Yb_{0.15}Lu_{0.85x}Y_{0.85-0.85x})_3Al_5O_{12}$ (x=0, 0.25, 0.5, 1) at two wavelengths (330 nm, 500 nm) were listed in Table 2. All values were relatively close in the range of 0.78 ns-1.34 ns, which are comparable to 0.41 ns excited by 266 nm pulsed laser in reference[5]. However, Nikl et al.[23] reported the 340 nm luminescence decay times of Yb:YAG and Yb:LuAG at 7 K, which were 75.8 ns and 51.4 ns, respectively, much longer than the fitting results in this paper. The reason is that the luminescence decay time shortened rapidly with increasing temperature, showing an obvious temperature quenching phenomenon[33]. The decay time of each wavelength for the four sample are less than 2 ns, indicating that the $(Yb_{0.15}Lu_{0.85x}Y_{0.85-0.85x})_3Al_5O_{12}$ single crystals have a good application prospect in ultrafast scintillation.

Besides, the decay time of the crystals for $(Yb_{0.15}Lu_{0.85x}Y_{0.85-0.85x})_3Al_5O_{12}$ shorten with the increasing of Lu^{3+} concentration, which shows a strong relationship. Therefore, we depict the decay time at 330 nm with the concentration of Lu^{3+} in FIG. 7 and fit the curve with Equation (4). The curve follows a quadratic function, and the adjusted R^2=0.99995. The trend of decay time is consistent with the XEL spectrum. The variation of these decay time may be related to the change of XEL intensity. Therefore, the crystal decay time and density can be smoothly tuned by Lu^{3+} concentration.

Table 2. The decay time constants of the single crystals for $(Yb_{0.15}Lu_{0.85x}Y_{0.85-0.85x})_3Al_5O_{12}$ (x=0, 0.25, 0.5, 1) at 330 nm and 500 nm wavelengths.

Wavelength (nm)	330 nm	500 nm
$(Yb_{0.15}Y_{0.85})_3Al_5O_{12}$	1.12 (ns)	1.34 (ns)
$(Yb_{0.15}Lu_{0.2125}Y_{0.6375})_3Al_5O_{12}$	1.11 (ns)	1.14 (ns)
$(Yb_{0.15}Lu_{0.425}Y_{0.425})_3Al_5O_{12}$	1.04 (ns)	1.02 (ns)
$(Yb_{0.15}Lu_{0.85})_3Al_5O_{12}$	0.78 (ns)	0.84 (ns)

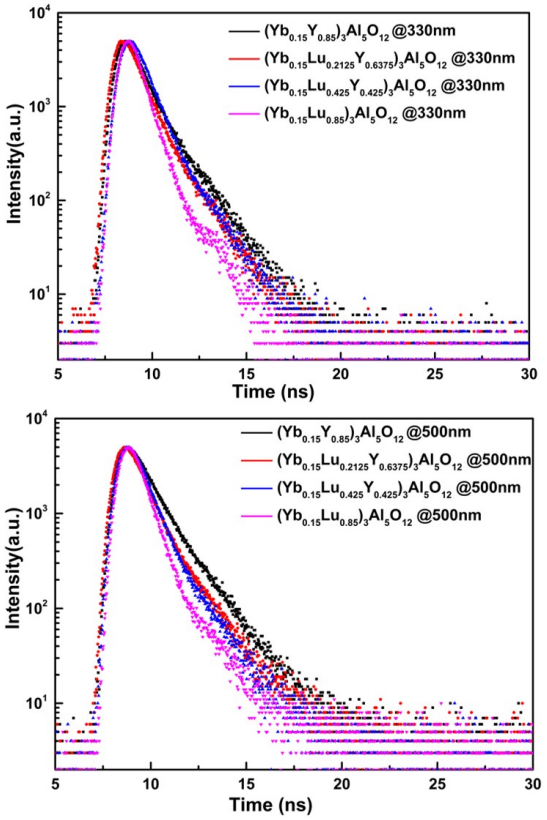

FIG. 6. Pulsed laser at 213 nm exited decay time at 330 nm, 500 nm profiles of the single crystals for $(Yb_{0.15}Lu_{0.85x}Y_{0.85-0.85x})_3Al_5O_{12}$ (x=0, 0.25, 0.5, 1).

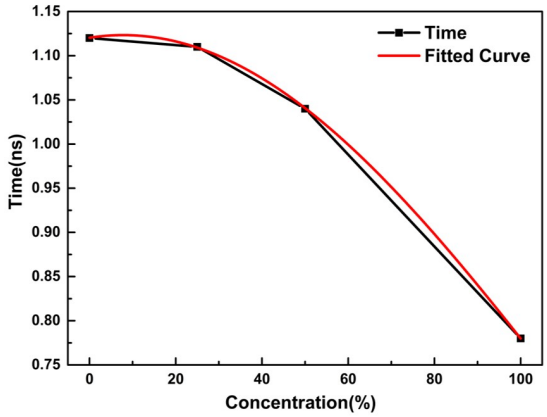

FIG. 7. Decay time of the single crystals for $(Yb_{0.15}Lu_{0.85x}Y_{0.85-0.85x})_3Al_5O_{12}$ (x=0, 0.25, 0.5, 1) at 330 nm with Lu^{3+} concentration increase.

$$y=exp(0.11+6.73\times10^{-4}\cdot x-4.3\times10^{-5}\cdot x^2) \quad (4)$$

4. Conclusions

The $(Yb_{0.15}Lu_{0.85x}Y_{0.85-0.85x})_3Al_5O_{12}$ (x=0, 0.25, 0.5, 1) crystals were obtained by the Cz method. The optical properties, XEL spectra and luminescence decay time of the Yb-doped YAG-LuAG solid solute system were analyzed in detail. Compared with the Yb:YAG, Lu^{3+} can effectively improve the effective atomic number and density of the crystal, which would have a better application prospect in the field of high intensity detection[34]. Besides, the XEL intensity and the luminescence decay time can be accurately regulated by the Lu:Y ratio, which provides flexible choice for different application scenarios.

Acknowledgments

This work was funded by the National Natural Science Foundation of China (Grant No. 52002386, 52072183, 51972319), the Shanghai Science and Technology Commission (Grant No. 20511107400) and the Youth Innovation Promotion Association, Chinese Academy of Science (CAS) (grant numbers 2021245).

References

1. M. Nikl, "Scintillation detectors for x-rays." Meas. Sci. Technol. **17**, R37 (2006).

2. M. Œwirkowicz, M. Skórczakowski, J. Jabczynski, A. Bajor, and E. Tymicki, "Investigation of structural, optical and lasing properties of YAG:Yb single crystals." Opto-Electronics Review **13**, 213 (2005).

3. L. Johnson, J. Geusic, and L. Van Uitert, "Coherent oscillations from Tm^{3+}, Ho^{3+}, Yb^{3+} and Er^{3+} ions in yttrium aluminum garnet." Applied Physics Letters **7**, 127 (1965).

4. Y. Zhao, Q. Wang, L. Meng, Y. Yao, S. Liu, N. Cui, L. Su, L. Zheng, H. Zhang, and Y. Zhang, "Anisotropy of the thermal and laser output properties in Yb,Nd:Sc_2SiO_5 crystal." Chin. Opt. Lett. **19**, 5 (2021).

5. Z. Li, D. Tang, J. Zhang, M. Hu, and Y. Chen, "Experimental Research on Time Response of Two Kinds of Yb^{3+}-Doped Scintillators Emission Spectra Excited by Laser." Atomic Energy Science and Technology **46**, 608 (2012).

6. K. Zhang, X. Ouyang, Z. Song, H. Han, Y. Zuo, X. Guan, X. Tan, Z. Zhang, and J. Liu, "An ideal scintillator–ZnO:Sc for sub-nanosecond pulsed radiation detection." Nucl. Instrum. Methods Phys. Res. Sect. A-Accel. Spectrom. Dect. Assoc. Equip **756**, 14 (2014).

7. X. Chen, Z. Zhang, K. Zhang, X. Guan, X. Weng, and H. Han, "Study on the time response of a barium fluoride scintillation detector for fast pulse radiation detection." IEEE Trans. Nucl. Sci. **67**, 1893 (2020).

8. M. Hu, Z. Li, Y. Fu, D. Tang, J. Zhang, J. Liu, R. Li, L. Chen, and Y. Huang, "The Measurement of Increase Yb:YAG Scintillation Detector Pulse Output Electric Charge." Nucl. Electron. Detect. Technol. **37**, 647 (2017).

9. K. Zhang, H. Hu, Z. Song, H. Han, X. Guan, Y. Lu, X. Chen, and Y. Yi, "Experiment investigation on pulsed gamma-ray fluence rate effect on Yb-doped yttrium aluminum garnet scintillator." Review of Scientific Instruments **92**, 063304 (2021).

10. R. S. Raghavan, "New prospects for real-time spectroscopy of low energy electron neutrinos from the sun." Phys. Rev. Lett. **78**, 3618 (1997).

11. L. van Pieterson, M. Heeroma, E. De Heer, and A. Meijerink, "Charge transfer luminescence of Yb^{3+}." J. Lumines. **91**, 177 (2000).

12. N. Guerassimova, N. Garnier, C. Dujardin, A.G. Petrosyan, and C. Pedrini, "X-ray excited charge transfer luminescence of ytterbium-containing aluminium garnets." Chem. Phys. Lett. **339**, 197 (2001).

13. P. Antonini, S. Belogurov, G. Bressi, G. Carugno, and P. Santilli, "Scintillation properties of Yb-doped yttrium-aluminum garnets." Nucl. Instrum. Methods Phys. Res. Sect. A-Accel. Spectrom. Dect. Assoc. Equip. **488**, 591 (2002).

14. W. Chewpraditkul, L. Swiderski, M. Moszynski, T. Szczesniak, A. Syntfeld-Kazuch, C. Wanarak, and P. Limsuwan, "Comparative studies of $Lu_3Al_5O_{12}$:Ce and $Y_3Al_5O_{12}$:Ce scintillators for gamma-ray detection." Phys. Status Solidi A-Appl. Mat. **206**, 2599 (2009).

15. C. Wanarak, A. Phunpueok, and W. Chewpraditkul, "Scintillation response of $Lu_{1.95}Y_{0.05}SiO_5$:Ce and Y_2SiO_5:Ce single crystal scintillators." Nucl. Instrum. Methods Phys. Res. Sect. B-Beam Interact. Mater. Atoms **286**, 72 (2012).

16. S. Belogurov, G. Bressi, G. Carugno, and Y. Grishkin, "Properties of Yb-doped scintillators: YAG, YAP, LuAG." Nucl. Instrum. Methods Phys. Res. Sect. A-Accel. Spectrom. Dect. Assoc. Equip. **516**, 58 (2004).

17. K. Mori, "Transient color-centers caused by UV light irradiation in yttrium aluminum garnet crystals." Phys. Status Solidi A-Appl. Res. **42**, 375 (1977).

18. D. Fagundes-Peters, N. Martynyuk, K. Lünstedt, V. Peters, K. Petermann, G. Huber, S. Basun, V. Laguta, and A. Hofstaetter, "High quantum efficiency YbAG-crystals." J. Lumines. **125**, 238 (2007).

19. C. Chen, G. Pogatshnik, Y. Chen, and M. R. Kokta, "Optical and electron-paramagnetic resonance studies of Fe impurities in yttrium aluminum garnet crystals." Phys. Rev. B **38**, 8555 (1988).

20. S. Rydberg, and M. Engholm, "Charge transfer processes and ultraviolet induced absorption in Yb:YAG single crystal laser materials." J. Appl. Phys. **113**, 6 (2013).

21. K. Li, S. Gan, G. Hong, and J. Zhang, "Relationship between crystal structure and luminescence properties of $(Y_{0.96-x}Ln_xCe_{0.04})_3Al_5O_{12}$ (Ln=Gd, La, Lu) phosphors." J. Rare Earths **25**, 692 (2007).

22. A. P. Anantharaman, and H. P. Dasari, "Potential of pyrochlore structure materials in solid oxide fuel cell applications." Ceram. Int. **47**, 22 (2021).

23. M. Nikl, A. Yoshikawa, and T. Fukuda, "Charge transfer luminescence in Yb^{3+}-containing compounds." Opt. Mater. **26**, 545 (2004).

24. Y. Fujimoto, M. Sugiyama, T. Yanagida, S. Wakahara, S. Suzuki, S. Kurosawa, V. Chani, and A. Yoshikawa, "Comparative study of optical and scintillation properties of Tm^{3+}:YAG, and Tm^{3+}:LuAG single crystals." Opt. Mater. **35**, 2023 (2013).

26. M. K. Ashurov, Y. K. Voronko, V. V. Osiko, A. A. Sobol, and M. I. Timoshechkin, "Spectroscopic study of stoichiometry deviation in crystals with garnet structure." Phys. Status Solidi A-Appl. Res. **42**, 101 (1977).

27. Y. Zorenko, and V. Gorbenko, "Growth peculiarities of the $R_3Al_5O_{12}$ (R=Lu, Yb, Tb, Eu–Y) single crystalline film phosphors by liquid phase epitaxy." Radiat. Meas. **42**, 907 (2007).

28. M. Nikl, E. Mihokova, J. Pejchal, A. Vedda, Y. Zorenko, and K. Nejezchleb, "The antisite Lu-Al defect-related trap in $Lu_3Al_5O_{12}$: Ce single crystal." Phys. Status Solidi B-Basic Solid State Phys. **242**, R119 (2005).

29. C. R. Stanek, K. J. Mcclellan, M. R. Levy, C. Milanese, and R. W. Grimes, "The effect of intrinsic defects on $RE_3Al_5O_{12}$ garnet scintillator performance." Nucl. Instrum. Methods Phys. Res. Sect. A-Accel. Spectrom. Dect. Assoc. Equip. **579**, 27 (2007).

31. Y. Zorenko, V. Gorbenko, I. Konstankevych, A. Voloshinovskii, G. Stryganyuk, V. Mikhallin, V. Kolobanov, and D. Spassky, "Single-crystalline films of Ce-doped YAG and LuAG phosphors: advantages over bulk crystals analogues." J. Lumines. **114**, 85 (2005).

32. Y. Kuwano, K. Suda, N. Ishizawa, and T. Yamada, "Crystal growth and properties of $(Lu,Y)_3Al_5O_{12}$." J. Cryst. Growth **260**, 159 (2004).

33. H. Ogino, A. Yoshikawa, J.H. Lee, M. Nikl, N. Solovieva, and T. Fukuda, "Growth and scintillation properties of Yb-doped $Lu_3Al_5O_{12}$ crystals." J. Cryst. Growth **253**, 314 (2003).

34. M. Nikl, A. Vedda, M. Fasoli, I. Fontana, V.V. Laguta, E. Mihokova, J. Pejchal, J. Rosa, and K. Nejezchleb, "Shallow traps and radiative recombination processes in $Lu_3Al_5O_{12}$: Ce single crystal scintillator." Phys. Rev. B **76**, 8 (2007).